

Performance evaluation of dimensionality reduction techniques on CHRIS hyperspectral data for surface discrimination

Veeramallu Satya Sahithi and Iyyanki V Murali Krishna

Research Centre Imarat (RCI-DRDO), Vigyana Kancha, Hyderabad – 500069

Email: sahithi.geo@gmail.com, iyyanki@gmail.com

(Received: Jun 19, 2015; in final form: Dec 31, 2015)

Abstract: Dimensionality reduction (DR) techniques help in reducing the volume of the hyperspectral data with minimum loss of information. The three most commonly used DR techniques – PCA, MNF and ICA have their own advantages and limitations in transforming the redundant hyperspectral data to non-redundant data thus aiding in an improved feature extraction. In the present work, an attempt was made to analyze the performance of hybrid dimensionality reduction method which uses a combination of three non – linear DR techniques for extracting the concrete materials from the CHRIS hyperspectral data. SAM and SID classifiers were used for classifying six different surface materials (concrete, paved and unpaved) in the study area along with four different vegetation types. Analysis has shown that the hybrid method gave satisfactory results for classifying the surface materials in CHRIS data. The SAM classifier gave the best results with an accuracy improvement of 10% after adapting the hybrid method. The classification accuracies have increased from 79.54% to 85.14% for SAM classification and 80.24% to 84.90% for SID classification.

Keywords: Principle component analysis(PCA), Minimum noise function (MNF), Independent component analysis (ICA), Hybrid method, Classification

1. Introduction

Hyperspectral data contain high spectral information due to the continuous spectral bands and narrow band width. Such high voluminous data may lead to redundant information. To overcome the problem of redundancy and for flexible feature extraction from the voluminous hyperspectral datasets, certain dimensionality reduction (DR) techniques are used. The dimensionality reduction techniques transform the data into a new domain where the data in each band is made uncorrelated to the other band based on certain criteria. There are many kinds of DR techniques that are broadly classified as linear and non – linear DR techniques. The three well known feature extraction/dimensionality reduction techniques include the principal component analysis (PCA), minimum noise fraction (MNF) and independent component analysis (ICA) techniques. Each of these techniques works on a unique principle and has its own advantages and disadvantages. Besides, each technique extracts unique features that are totally different to that others extract. The PCA techniques works on the data variance, MNF sorts the information based on the SNR

and the ICA assumes each band to be a linear mixture of some independent hidden components and thus applies a linear unmixing procedure to extract the independent features. PCA and MNF measure the second order statistics of the data with a gaussian assumption, while ICA uses higher order statistics and gives statistically independent components with non – gaussian assumption (Wang et.al., 2014). The second order statistics used in PCA and MNF cannot uncover the subtle material substances that are uncovered by hyperspectral images (Wang et.al., 2014). Hence, to make the most out of each of these techniques and to overcome their disadvantages, Galal and Hasan, 2012, in his paper “Learning Flexible Hyperspectral Features” proposed an improved method of feature extraction, where a combination all the three

unsupervised DR techniques is used to extract the features of interest. Initially an MNF transform was applied on AVIRIS hyperspectral data and the bands containing the highest signal to noise ratio (SNR) were considered for the next step. In the next step, the first 10 MNF bands containing high SNR were used as inputs for PCA and ICA and the outputs of these transformations were stacked together to form a new vector for each pixel in the image. Each of these vectors was then classified using a Support Vector Machine. The method proposed in Galal and Hasan (2012) improved the overall performance of the SVM classifier and gave good results statistically. In the present work, the performance of this method was tested on a hyperspectral CHRIS image for extracting various concrete structures. The objective of the present study is to extract different kinds of concrete materials from dimensionally reduced the CHRIS hyperspectral image.

1.1. Principal Component Analysis (PCA)

PCA, also called the Karhunen-Love transform (KLT) or the Hotelling transform, is a classical statistical technique used to reduce the dimensionality of the multi-dimensional data. PCA finds a new set of orthogonal axes that have their origin at the data mean and that are rotated to maximize the data variance. The covariance matrix which is used as a transformation matrix is defined as:

$$\sum cov = \sum_{i=1}^n (\bar{x}_i - \bar{m}) (\bar{x}_i - \bar{m})^T \quad (1)$$

where \bar{x}_i is the i^{th} spectral value, \bar{m} is the mean spectral values, n is the number of pixels in the image. The eigen decomposition of the covariance matrix is performed in order to calculate the new orthogonal axes, which can be given as:

$$\sum \hat{a}_k = \lambda_k \hat{a}_k \quad ; k=1,2,\dots,N \quad (2)$$

where λ_k is the k^{th} eigen value, \hat{a}_k is the corresponding eigenvector and N being the number of bands. The eigen vector forms the axes of PCA space while the eigen values

are the measure of variance of the corresponding eigenvector. The information content of the band increases with the increasing value of variance (Panwar et al., 2014). The PCA bands are arranged based on the variance value – first band contains highest information with a largest eigen value, the second PC band contains the second largest amount of information and is orthogonal to the first PC, the third PC has the third largest variance value and is orthogonal to both first and second PC's and so on.

1.2. Minimum Noise Fraction (MNF)

MNF is one of the most commonly adopted unsupervised DR techniques for the hyperspectral data. The MNF transform is specifically designed as a linear transformation that maximizes the signal-to-noise ratio, thus ordering images in terms of decreasing image quality in lower order components. The foundations of the MNF transform were developed by Green *et al.* (1988) and Lee *et al.* (1990). The former explained it based on signal to noise ratio and demonstrated noise filtering via complex matrix inversion. Lee *et al.* (1990) simplified this as a two-cascaded PCA transform. The first phase of the MNF transform starts with image noise determination and noise covariance matrix calculation of the image which is subsequently followed by eigen value decomposition. The third step includes image mean correction, noise decorrelation and finally normalization of the linear noise in the data which is called as noise whitening (Mundt et al., 2007). This noise whitened data is decorrelated using a PCA transform which is the second step of MNF transform. The higher order images will have high SNR which gradually reduces towards the lower order images (which are noise dominated). Transformed MNF data are highly decorrelated and have zero mean and a unit noise variance. The covariance matrix of an MNF transformed dataset is a diagonal matrix with elements equal to the MNF eigen values.

1.3. Independent component Analysis (ICA)

ICA on multispectral or hyperspectral datasets transform a set of mixed random signals into components that are mutually independent. The major advantage of this ICA transform over PCA and MNF methods is that it is based on the non-Gaussian assumption of the independent sources which is a typical characteristic of hyperspectral datasets. It uses higher-order statistics to discover some interesting features in non-Gaussian hyperspectral datasets (Yusuf and He, 2011). IC transformation can distinguish features of interest even when they occupy only a small portion of the pixels in an image while in PCA these small features are buried in the noisy bands (ENVI 2010). Hence ICA analysis is very much helpful in spectral unmixing, anomaly and target detections.

ICA is a blind source separation technique. It assumes that each band is a linear mixture of independent hidden component and extracts the independent feature using a linear unmixing operation (Panwar et al., 2014).

Suppose we have N statistically independent signals, $s_i(t)$, $i=1, \dots, N$. let $X(t)$ denote the original source signal. ICA estimates $X(t)$ by,

$$s(t) = U X(t) \quad (3)$$

where U is an unknown matrix called the unmixing matrix. This is a blind source separation algorithm since we do not have any prior information about unmixing matrix or even on the source themselves.

2. Datasets and study area

The dataset used for the present study is the hyperspectral Compact High Resolution Imaging Spectrometer (CHRIS) on board the Proba mission of the European Space Agency. CHRIS is an experimental satellite which monitors the earth in five modes and in five different look angles - $+55^\circ$, $+36^\circ$, 0° , -36° and -55° (Sahithi and Agrawal, 2014). The image considered is a nadir (0°) looking image obtained in mode 5 (land use/land cover applications). It has a spatial resolution of 17m with 18 spectral bands in the range of 400 – 1500nm. The present study area is one of the test sites of CHRIS experimental sensor. The study area is a part of Suratgarh airbase station located in Sri Ganganagar district, Rajasthan. It falls within the latitude and longitude of $29^\circ 22' 24''\text{N}$ to $29^\circ 24' 49''\text{N}$ and $73^\circ 52' 44''\text{E}$ to $73^\circ 55' 54''\text{E}$. It has a total area of the airbase and is mostly composed of different concrete materials and two to three kinds of vegetation. A location map of the study area is given in Fig 1.

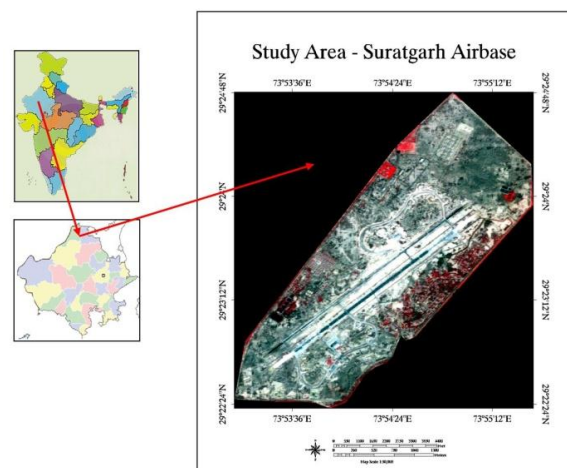


Figure 1: Study area used - LISS IV image of Suratgarh airbase, Rajasthan, India

3. Methodology

The radiometrically and atmospherically corrected CHRIS data is first reduced using the MNF transformation. The MNF components having high information are considered for further analysis. A principal component transformation and independent component analysis is performed over the selected MNF components which gave a set of components for each of these transformations. All these components are then stacked to form a new vector for each pixel in the image.

A simple SAM (Spectral Angle Mapper) classifier and Spectral Informed Divergence (SID) classifier are used over this stacked image to classify various surface materials in the study area. Total of 10 classes were considered - new concrete, old concrete, tar, white paint, sand, cemented area, croplands, shrubs, thorny trees,

bushy trees. The average spectra of various materials considered for classification are shown in Fig 3. A constant SAM angle of 0.15 was used for classifying the final hybrid DR reduced image and the original CHRIS image.

Observations were made to trace some inherent features which are not observed in CHRIS original hyperspectral image. The extracted features after classification are validated using the temporal google earth images.

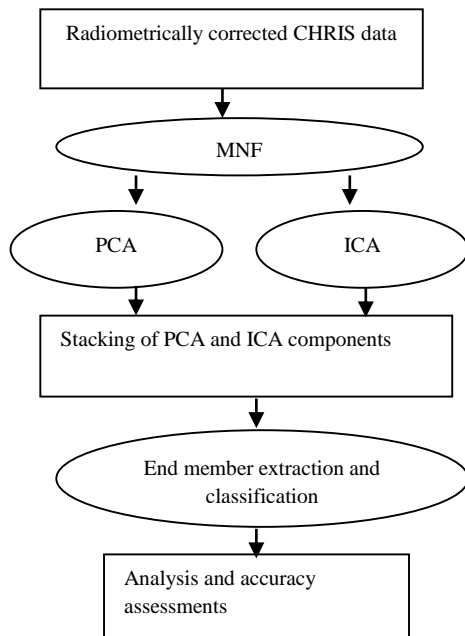


Figure 2: Methodology

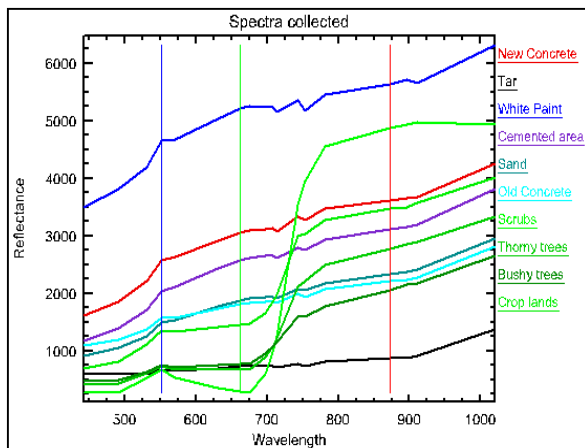


Figure 3: Average spectra of various materials collected for classification

4. Results and analysis

On performing the MNF transform over the CHRIS image, the first 8 bands are considered for further processing due to their high signal to noise ratio. The components were chosen based on their eigen value and visual information content. Apart from the MNF transform, a simple PCA and ICA are also applied over the hyperspectral image to test the performance of various dimensionality reduction techniques. The eigen values of PCA, MNF and ICA

transformations of the hyperspectral image are shown in table 1. The components having the highest eigen values are considered as the informative bands and hence the first 8 bands are considered in this work. The huge difference in the eigen values of first and second PCA component shows the diversity in information content and non-correlation between the adjacent bands. Visual inspections have shown that independent component analysis had more noise. An observation was made on the eigen values of PCA, MNF and ICA transformations which showed that PCA and ICA had similar eigen values. This was due to the fact that ICA is a two step process which starts with an initial PCA transform of the image. PCA and ICA transforms performed on the MNF components produced better results than the direct PCA and ICA results.

Table 1: The eigen values of PCA, MNF and ICA transformations

Band number	PCA after MNF	ICA after MNF	MNF Eigen values
1	79.764	79.764	79.764
2	10.259	10.259	10.259
3	7.670	7.670	7.670
4	5.995	5.995	5.995
5	3.626	3.626	3.626
6	3.284	3.284	3.284
7	2.519	2.519	2.519
8	2.309	2.309	2.309

However, the eigen values of the PCA post MNF and ICA post MNF were same (Table 2) over the original CHRIS image.

Table 2: The eigen values of PCA after MNF, MNF and ICA after MNF transformations

Band number	PCA Eigen Values	MNF Eigen values	ICA Eigen Values
1	23439699.36	79.765	23439699.36
2	174555.788	10.260	174555.788
3	8415.922	7.671	8415.923
4	5898.305	5.995	5898.305
5	625.206	3.626	625.206
6	551.119	3.284	551.119
7	340.441	2.519	340.441
8	208.063	2.3094	208.063

The stacked image obtained by laying the PCA post MNF components over the ICA post MNF components was used for classification of various surface materials. Supervised SAM and SID classifications were used for surface material classification over the stacked image and the original atmospherically corrected CHRIS nadir image. A comparative study of classified stacked image and the classified original image for six different concrete (paved and unpaved) surfaces have shown that the considered method yielded better classification results than the original image. The DR techniques not only helped in reducing the size of the input image but also removed the

unwanted and redundant noise from the image. This technique highlighted certain hidden man made concrete features like roads, houses etc.

The removal of unwanted noise from the bands improved the results of SAM classification. Thin structures like road path, smaller concrete structures etc which were poorly classified in the original hyperspectral image were well classified after using the stacked vector. The overall accuracies improved by 5 to 6% after using this

methodology. Some of the positive visual observations noticed using the classification results are shown in the following figures. The classification of the stacked image extracted the roads in the airbase more distinctly than the classification of the original CHRIS image. Improvements in the extraction of road structures and curved paths are shown in Fig 6.

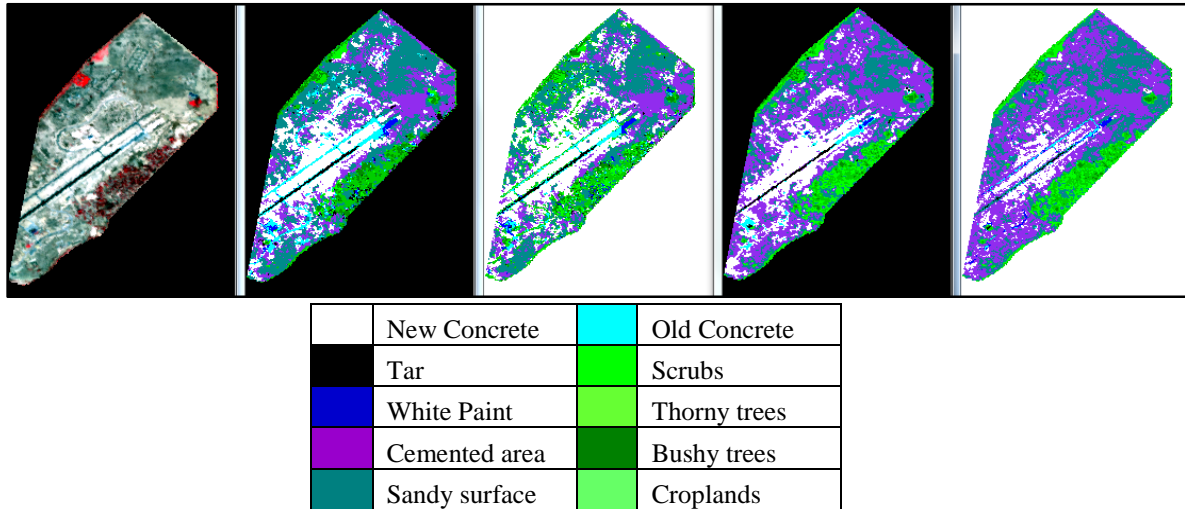


Figure 4: Classification of Stacked image (PCA after MNF and ICA after MNF) and the CHRIS atmospherically corrected image using SAM and SID classifiers

Table 3: Classification accuracies of various surface materials considered in classification

Class name	Spectral Angle Mapper		Spectral Informed Divergence	
	Original CHRIS	Stacked Vector	Original CHRIS	Stacked Vector
New Concrete	78.56%	85.25%	79.56%	87.67%
Tar	85.45%	87.63%	84.68%	88.65%
White Paint	88.56%	91.58%	89.25%	91.44%
Cemented area	72.66%	85.86%	73.58%	80.25%
Sandy surface	74.56%	84.78%	81.21%	82.56%
Old Concrete	80.45%	87.45%	81.56%	87.24%
Scrubs	81.25%	83.15%	79.54%	81.45%
Thomy trees	75.45%	77.63%	74.68%	78.65%
Bushy trees	79.21%	83.47%	80.12%	84.65%
Croplands	79.25%	84.56%	78.21%	86.46%
Average accuracy	79.54%	85.14%	80.24%	84.90%

Accuracy assessment was performed over the four classified images - SAM classified original and transformed stacked images, SID classified original and transformed stacked images. The accuracies for each class in all the four classified maps are shown in table 3. Both

SAM and SID classifiers had equal performance in classification. A SAM angle of 0.15 was used for classification of both the original and transformed images. The overall average accuracies (Fig. 5) have increased from 79.54% to 85.14% for SAM classification and 80.24% to 84.90% for SID classification.

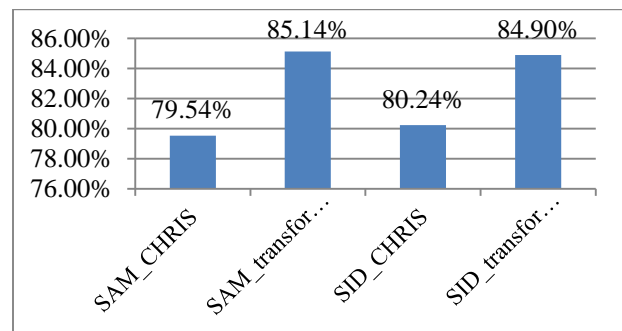


Figure 5: Overall classification accuracies

The spatial resolution of the hyperspectral image plays a major role in the image classification, apart from its high spectral resolution. In the present work, the spatial resolution of 17m of the CHRIS hyperspectral image is still coarse to misclassify the pixel into a different class (mixed pixel effect).

Also it is accepted that the transformed image could not completely restore the spectral resolution of the original CHRIS image after using the DR techniques. Hence, a compromise in the overall accuracy rate of the classifiers is accepted.

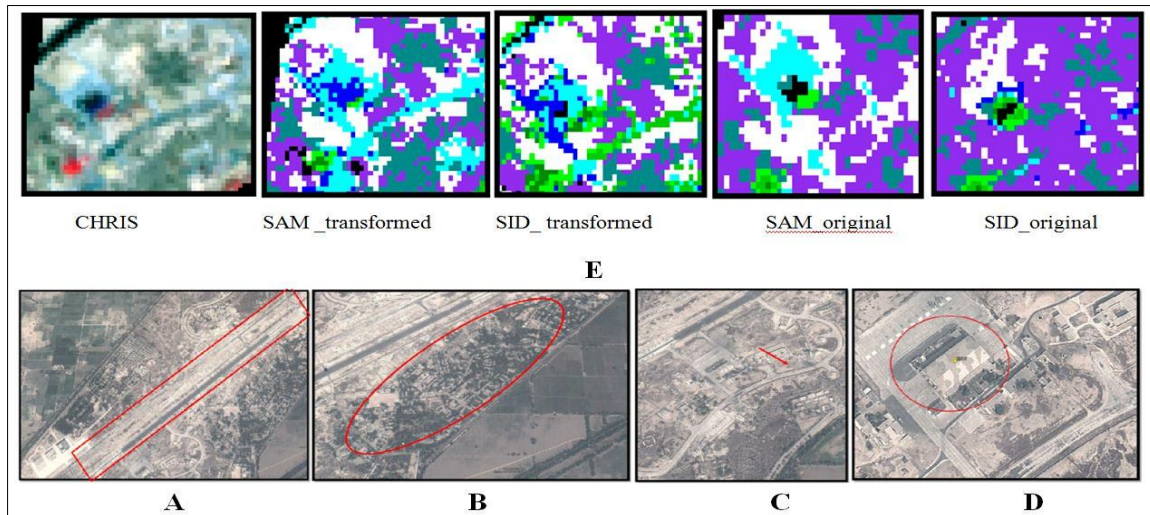


Figure 6: A - Improvements in the extraction of road paths up on classification; B - Improvements in the extraction of urban and concrete buildings in a township; C - Extraction of curved path; D - Extraction of building roof coated with artificial paints; E - Google Earth images of figures – A, B, C, D respectively

5. Conclusions

In this paper, an existing methodology was tested in extracting the features from dimensionally reduced CHRIS hyperspectral data. The MNF technique helped in extracting the data with high signal to noise ratio and in removing the noisy bands from the voluminous hyperspectral data. PCA and ICA transformation of the transformed MNF components helped in bringing out some features which could not be directly observed in the atmospherically corrected untransformed hyperspectral data. ICA technique disclosed the spectral differences in a patch of mixed urban and vegetation. The PCA technique de-correlated the MNF transformed data and some features like roads and other structures hidden within the various bands of the CHRIS image were revealed after this transform. On the whole a combined method of MNF, PCA and ICA techniques seemed to be of great use in detecting the smallest information present in the hyperspectral data. The performance of SAM classifier ameliorated on using the transformed non-redundant and decorrelated data showing a significant improvement in the classification accuracies.

Acknowledgement

The authors are thankful to Dr Sateesh Reddy, the outstanding scientist and Director, Dr BV Rao, Technology Director, Dr Arindan Biswas, Scientist from IIRS and Rama Sarma, DOMS, RCI, DRDO for their interest and for providing the necessary infrastructure and extending all support whenever required.

References

Galal, A. and H. Hasan (2012). Learning Flexible Hyperspectral Features. *International Journal of Remote Sensing Applications*. IJRSA Vol.2 Iss. 2, 44-48

Green, A.A., M. Berman, P. Switzer and M.D. Craig (1988). A transformation for ordering multispectral data in

terms of image quality with implications for noise removal. *Transactions on Geoscience and Remote Sensing*, 26(1), 65-74.

Lee, J.B., S. Woodyatt and M. Berman (1990). Enhancement of high spectral resolution remote sensing data by a noise-adjusted principal components transform. *IEEE Transactions on Geoscience and Remote Sensing*, 28(3), 295-304.

Mundt, J.T., D.R. Streutker and F.G. Nancy (2007). Partial unmixing of hyperspectral imagery: Theory and methods. *Proceedings of the American Society of Photogrammetry and Remote Sensing*.

Panwar, A., A. Singh and H.S. Bhaduria (2014). *International Journal of Emerging Technology and Advanced Engineering*. ISSN 2250-2459, ISO 9001:2008 Certified Journal, Volume 4, Issue 5, 701 - 705.

Sahithi, V.S. and S. Agrawal (2014). Sub pixel location identification using super resolved multilooking CHRIS data. *ISPRS-International Archives of the Photogrammetry, Remote Sensing and Spatial Information Sciences*, 1, 463-468.

Tutorial, E.Z. (2010). *ENVI user guide*. Colorado Springs, CO: ITT.

Wang, Y., G. Wu and L. Ding (2014). Plant Species Identification Based on Independent Component Analysis for Hyperspectral Data. *Journal of Software* 9.6: 1532-1537.

Yusuf, B.L. and Y. He (2011). Application of hyperspectral imaging sensor to differentiate between the moisture and reflectance of healthy and infected tobacco leaves. *African Journal of Agricultural Research*, 6(29), 6267-6280.